Brain Advance Access published November 24, 2015

BRAIN
A JOURNAL OF NEUROLOGY

REPORT

Early detection of intentional harm in the human amygdala

Eugenia Hesse,[1,2,3,*] Ezequiel Mikulan,[1,2,4,*] Jean Decety,[5] Mariano Sigman,[6,7] María del Carmen Garcia,[8] Walter Silva,[8] Carlos Ciraolo,[8] Esteban Vaucheret,[8] Fabricio Baglivo,[1,2,3] David Huepe,[2] Vladimir Lopez,[9] Facundo Manes,[1,2,4,10] Tristan A. Bekinschtein[11] and Agustin Ibanez[1,2,4,10,12]

*These authors contributed equally to this work.

A decisive element of moral cognition is the detection of harm and its assessment as intentional or unintentional. Moral cognition engages brain networks supporting mentalizing, intentionality, empathic concern and evaluation. These networks rely on the amygdala as a critical hub, likely through frontotemporal connections indexing stimulus salience. We assessed inferences about perceived harm using a paradigm validated through functional magnetic resonance imaging, eye-tracking and electroencephalogram recordings. During the task, we measured local field potentials in three patients with depth electrodes ($n = 115$) placed in the amygdala and in several frontal, temporal, and parietal locations. Direct electrophysiological recordings demonstrate that intentional harm induces early activity in the amygdala (<200 ms), which—in turn—predicts intention attribution. The amygdala was the only site that systematically discriminated between critical conditions and predicted their classification of events as intentional. Moreover, connectivity analysis showed that intentional harm induced stronger frontotemporal information sharing at early stages. Results support the 'many roads' view of the amygdala and highlight its role in the rapid encoding of intention and salience—critical components of mentalizing and moral evaluation.

1 Laboratory of Experimental Psychology and Neuroscience, Institute of Cognitive Neurology, Favaloro University, Buenos Aires, Argentina
2 UDP-INECO Foundation Core on Neuroscience (UIFCoN), Faculty of Psychology, Universidad Diego Portales, Santiago, Chile
3 Instituto de Ingeniería Biomédica, Facultad de Ingeniería, Universidad de Buenos Aires, Argentina
4 National Research Council (CONICET), Buenos Aires, Argentina
5 Department of Psychology, and Department of Psychiatry and Behavioural Neuroscience, The University of Chicago, Chicago, IL, USA
6 Laboratory of Neuroscience, Universidad Torcuato Di Tella, Buenos Aires, Argentina
7 Departamento de Física, FCEN, UBA and IFIBA, Conicet, Buenos Aires, Argentina
8 Programa de Cirugía de Epilepsia, Hospital Italiano de Buenos Aires, Buenos Aires, Argentina
9 Escuela de Psicología, Pontificia Universidad Católica de Chile, Santiago, Chile
10 Centre of Excellence in Cognition and its Disorders, Australian Research Council (ARC), New South Wales, Australia
11 Department of Psychology, University of Cambridge, Cambridge, UK
12 Universidad Autónoma del Caribe, Barranquilla, Colombia

Correspondence to: Agustin Ibanez,
Laboratory of Experimental Psychology and Neuroscience,
Institute of Cognitive Neurology,
Favaloro University, Buenos Aires, Argentina
E-mail: aibanez@ineco.org.ar

Keywords: amygdala; intentional harm; moral cognition; intracranial recordings

Abbreviation: wSMI = weighted Symbolic Mutual Information

Received June 16, 2015. Revised September 22, 2015. Accepted September 25, 2015.

Introduction

Perceiving and reacting to harm is crucial for survival and social interaction. Indeed, the assessment of deliberately harmful actions moulds human morality (Decety *et al.*, 2012; Treadway *et al.*, 2014; Ames and Fiske, 2015). Moral evaluation engages neurocognitive mechanisms supporting theory of mind, intentionality, empathic concern and evaluation (Moll *et al.*, 2005; Young *et al.*, 2007; Moll and Schulkin, 2009; Decety and Cowell, 2014). Neuroimaging studies show that these cognitive domains involve widely distributed networks (Moll and Schulkin, 2009; Decety *et al.*, 2012; Ibanez and Manes, 2012). This network relies on the amygdala as a critical hub (Treadway *et al.*, 2014), likely through frontotemporal connections indexing stimulus salience (Pessoa and Adolphs, 2010).

However, available evidence presents various limitations. First, functional MRI studies of morality are blind to early differences among relevant mechanisms (Huebner *et al.*, 2009). Second, amygdala activation is confounded by stimulus-related signal fluctuation in nearby veins draining distant brain regions (Boubela *et al.*, 2015). Third, EEG/MEG studies of subcortical source space are inaccurate. Thus, no evidence exists of a direct and early involvement of the amygdala in the detection of intentional harm.

To bridge these gaps, we assessed inferences about perceived harm using a paradigm previously validated through functional MRI and eye-tracking (Decety *et al.*, 2012) as well as EEG recordings (Decety and Cacioppo, 2012; Escobar *et al.*, 2014). Participants viewed short videos depicting interactive situations that involved intentional harm, unintentional harm or no harm at all. Their task was to evaluate whether the actions were intentional or unintentional. All stimuli were presented in a three-frame sequence (T1: 500 ms, T2: 200 ms, T3: 1000 ms; see 'Materials and methods' section).

Materials and methods

Participants

Three patients with intractable epilepsy who were offered surgical intervention to alleviate their condition took part in the study. Subject 1 was a 19-year-old, right-handed female who had completed 1 year of tertiary education and suffered from drug-resistant epilepsy since the age of 16 years. Subject 2 was a 57-year-old, left-handed male with an undergraduate degree who suffered from drug-resistant epilepsy since the age of 42 years. Subject 3 was a 29-year-old, left-handed female with an undergraduate degree who suffered from epilepsy since the age of 18 years. All of the subjects gave written informed consent in accordance with the Declaration of Helsinki, and the study was approved by the Institutional Ethics Committee of the Hospital Italiano de Buenos Aires, Argentina. They were attentive and cooperative while performing the task. Their cognitive performance under the task was accurate (Supplementary Table 1).

Patients' recordings

Direct cortical recordings were obtained from semi-rigid, multi-lead electrodes that were implanted in each patient. The electrodes used have a diameter of 0.8 mm and consist of 5, 10 or 15 contact leads 2-mm wide and 1.5-mm apart (DIXI Medical Instruments). The video-SEEG monitoring system (Micromed) records as many as 128 depth-EEG electrode sites simultaneously. Our three subjects had electrodes in the left amygdala, although two of them were left-handed. No data were collected from the right amygdala. All patients were carefully selected such that the amygdalae from which the recordings were obtained were distal to the epileptogenic foci, and no single recording site presented epileptogenic activity (see below). Subject 1 had 128 sites recorded. Subject 2 had 90 sites recorded. Subject 3 had 105 sites recorded. The recordings were sampled at 1024 Hz.

Post-implantation MRI and CT scans were obtained from each patient. Both volumetric images were affine registered and normalized using the SPM8 MATLAB toolbox. Using MRIcron, the MNI coordinates of each contact site and their respective Brodmann areas were obtained and are listed in Supplementary Table 2. We used the normalized position of the electrodes' contact sites to an MNI coordinate space because this procedure allowed us to define the patient's results in a common space (Foster *et al.*, 2015).

Experimental design: task and stimuli

We used an adaptation of the Intention Inference Task (Decety *et al.*, 2012; Decety and Cacioppo, 2012; Escobar *et al.*, 2014) to assess the detection of intentional harmful actions. The task evaluates intentional detection in the context of intentional/unintentional/neutral harms and consists of three scenarios: (i) intentional harm in which one person is in a painful situation intentionally caused by another (e.g. pushing someone off a bench); or (ii) unintentional harms in which one person is in a painful situation unintentionally caused by another; and (iii) neutral or control situations (e.g. one person receiving a flower given by another). The Intention Inference Task evaluates the comprehension of the unintentional or deliberate nature of the action and the intention of the perpetrator to hurt. It consists of 25 animated scenarios (11 intentional, 11 unintentional, three neutral), and one practice trial for each category (before the task). The patients were asked to perform the task a few times. Subjects performed the task twice (Subject 2 three times). Although these are a small number of trials, our results were robust and were consistent with the single trial responses observed in intracranial recordings and their enhanced signal-to-noise ratio (Jacobs and Kahana, 2010). Each scenario consists of three digital colour pictures presented in a successive manner to imply motion. The durations of the first, second and third pictures in each animation were 500 (T1), 200 (T2), and 1000 (T3) ms, respectively. See the Supplementary material for stimuli validation with behavioural and eye-tracking measures. For additional stimulus examples and validation information, see Fig. 1A, Supplementary Fig. 1 and Supplementary material. For a video illustration of the clips, see Supplementary Video 1.

The faces of the protagonists were not visible and thus there were no facial emotional reactions visible to the patients. However, body expressions and postures provided sufficient

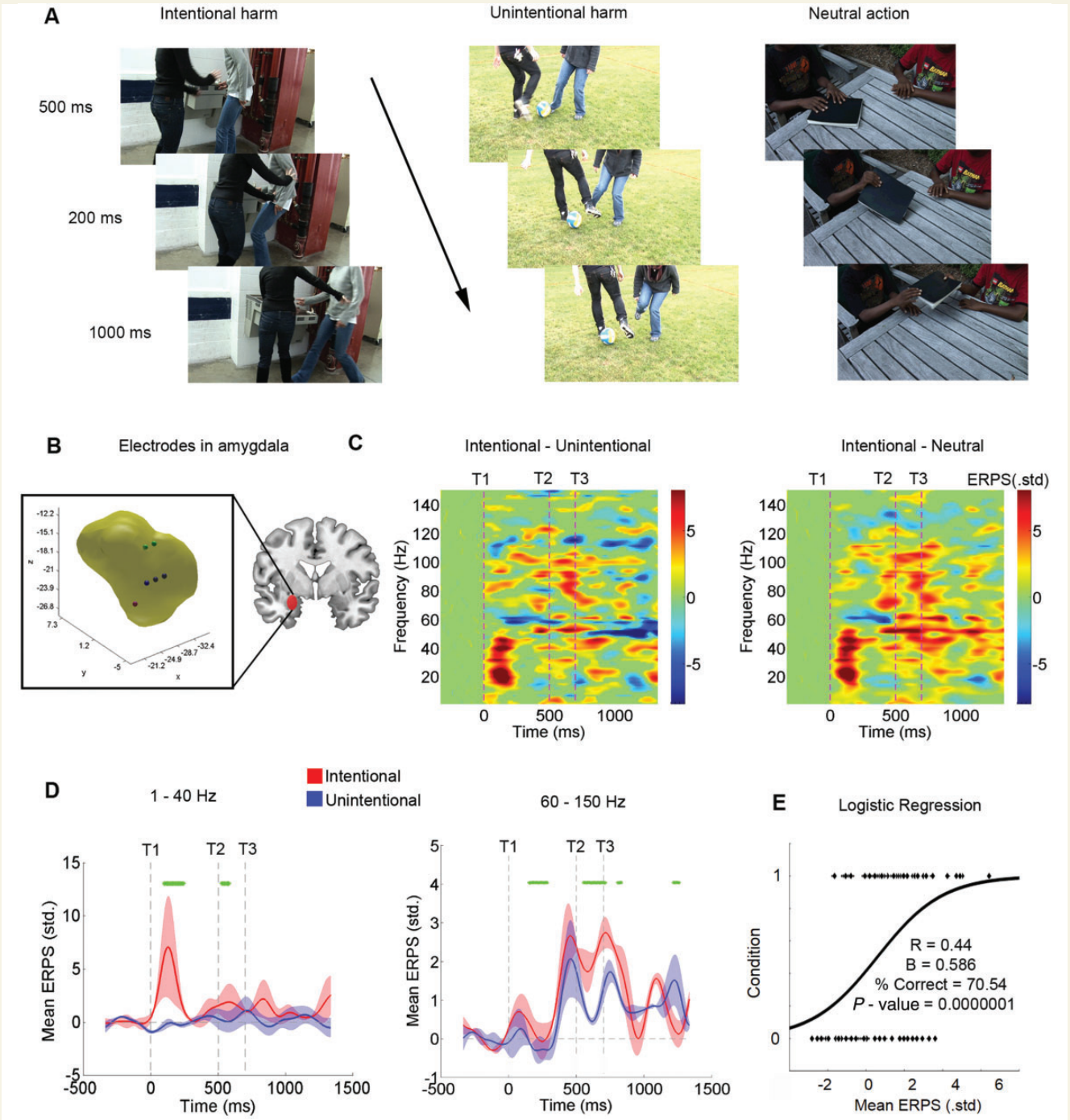

Figure 1 Amygdala responses to intentional harm. (**A**) Examples of stimuli used for intentional, unintentional, and neutral conditions, together with the temporal duration of each image (see examples in Supplementary Video 1). (**B**) Electrode contact sites in the amygdala. (**C**) Time-frequency charts. T1, T2 and T3 represent the times at which each digital picture is presented to the subject. A zero value was assigned to points that were not significant ($P > 0.05$) relative to the baseline. *Left*: Subtraction between the amygdala time-frequency charts obtained from the intentional and unintentional conditions. *Right*: Subtraction between the amygdala time-frequency charts obtained from the intentional and neutral conditions. (**D**) Averaged power spectrum of the intentional and unintentional time-frequency charts using different frequency ranges. The green marks identify significant differences between conditions (bootstrapping, $P < 0.01$). *Left*: Frequency range 1–40 Hz. *Right*: 60–150 Hz. (**E**) Binary logistic regression between conditions (intentional = 1, unintentional = 0) and mean value of the power spectrum on broadband and 0–1000 ms window (B = 0.580, R = 0.44, $P = 0.0000001$, correct categorization = 70.54%).

information about the intention of the agent. Patients were asked to respond to intentionality (was the harmful action done on purpose?). The question was answered by selecting 'Yes' or 'No' with two different buttons.

Data analysis

Signal preprocessing

The data were bandpass filtered from 1 to 200 Hz using a zero phase shift finite impulse filter. Then, they were notch filtered at 50 Hz and its harmonic frequencies (100 Hz, 150 Hz) to eliminate the line artefacts. The contact sites recorded from each patient who presented artefacts and pathological waveforms were discarded. This was achieved by visually inspecting the recordings and by the following criteria: (i) signal values do not exceed five times the signal mean; and/or (ii) consecutive signal samples do not exceed 5 standard deviations (SD) from the gradient mean. A total number of 115 contact sites remained after applying these criteria (35 contact sites for Subject 1, 44 for Subject 2 and 36 for Subject 3; Supplementary Fig. 2).

Once the sites that complied with the criteria were selected, they were referenced to the mean value (the averages of the sites per subject were subtracted from each recording). Finally, the data were segmented into 2000 ms epochs, including a −500 to 0 ms prestimulus baseline period. The epochs were baseline corrected.

Time–frequency analysis

The time–frequency charts were obtained by analysing the digitized signals using a windowed Fourier transform (window length: 250 ms, step 8 ms, window overlap 97%) (Gross, 2014). Our scripts were based on the newtimef.m script. As the frequency analysis is window-centred, we consider that the earliest unbiased significant temporal value is ∼125 ms, when the window centre is at 0 ms (T1 stimulus presentation, see Supplementary material). The time–frequency charts were normalized to the baseline before the stimulus onset. The normalization involved subtracting the baseline average and dividing by the baseline standard deviation on a frequency-by-frequency basis using a window from −500 to 0 relative to the stimuli onset.

We obtained the time–frequency chart for each condition (intentional, unintentional and neutral harmful actions) and performed subtractions between them (intentional − unintentional, intentional − neutral and unintentional − neutral). Significant power increases and decreases across time against baseline values were analysed with Monte Carlo permutation tests (5000) combined with bootstrapping, as reported in other intracranial studies (Naccache *et al.*, 2005; Ibanez *et al.*, 2013). This simple method offers a straightforward solution for multiple comparison problems and for data distribution assumptions. Frequency band ranges of 1 to 40 Hz and broadband (60 to 150 Hz) of the time-frequency charts were averaged for the signals obtained from the intentional and unintentional conditions.

Logistic regression of the trial-by-trial analysis

Logistic regression analysis was performed to evaluate whether the power activity across each trial could predict the subject categorization as intentional or unintentional. The dependent variable was the unintentional (0) or intentional (1) condition. The independent variable of interest was the averaged value of power spectrum over time (0–1000 ms since stimuli onset) for the 60–150 Hz frequency range in each trial. Statistical significance was considered to be $P < 0.01$. Outliers were detected using the Tukey two-sided method (Tukey hinge distance factor = 1.5) (Tukey, 1977). Three outlier values were detected and left out of the analysis. This procedure was done for the amygdala power spectrum values and for the other regions, grouped by regions of interest within subjects (see below).

Comparison between the amygdala and the other regions

To assess the amygdala's power activation and ability to distinguish between conditions (logistic regression) relative to the other regions, we performed a three-step analysis: (i) to evaluate whether the region discriminates the intentional condition, and the intentional from unintentional conditions; (ii) to compare the amygdala's power activation with that of the regions that did discriminate the intentional conditions and the intentional from unintentional conditions; and (iii) to perform a logistic regression of single trial data as predictors of subject classification. See Supplementary material for detailed information on this three-step analysis.

Amygdala connectivity analysis using the weighted Symbolic Mutual Information measure

To analyse the amygdala's connectivity with the other regions within each subject, we used the weighted Symbolic Mutual Information (wSMI) measure (King *et al.*, 2013). This method calculates a non-linear index of information sharing between two signals. The signals are transformed into symbols. By defining a value of k, the number of samples that represent a symbol, and τ, the temporal separation between them, a frequency range is defined for which wSMI will be sensitized. The joint probability between the signals was then calculated for each pair of channels, for each trial, with a fixed value of k = 3 and τ = 32 ms—hence establishing the frequency range to 1–10 Hz. The

signals were low-pass filtered at 10 Hz to avoid aliasing effects (see Supplementary material for more details).

A seed analysis based on the wSMI was calculated for the amygdala's signal with the other regions within each subject for the intentional and unintentional conditions (signals without the baseline time window). The statistical comparisons between the connectivity values obtained for each condition were performed using a Wilcoxon Signed Rank test. The null hypothesis was rejected if a *t*-value was greater than the most extreme 5% of the distribution (i.e. $P < 0.05$). The BrainNet Viewer toolbox was used for visualization of wSMI.

Brief time span functional connectivity

A functional connectivity analysis (Omigie *et al.*, 2015) of the early window (0 to 500 ms) was implemented to study the correlation between different regions. The signals were first bandpass filtered in two frequency band ranges, 1 to 40 Hz and 60 to 150 Hz, for the intentional and unintentional signals. See Supplementary material for more details.

Results

During the task, we measured local field potentials (at T1, T2, and T3) in three patients (Subjects 1, 2 and 3) with depth electrodes ($n = 115$) placed in the amygdala (Fig. 1B, $n = 6$) and in several frontal, temporal and parietal locations ($n = 109$; see Supplementary Fig. 2 and Supplementary Table 2 for spatial locations).

Intentionality and content (harm versus neutral) were discriminated by an activity boost in the amygdala (all sites). This was observed during the first 200 ms after stimulus onset (T1) at 1–40 Hz and throughout T1–T2–T3 at broadband (60–150 Hz) (Fig. 1C and Supplementary Fig. 3). Bootstrapped permutations of single trial analysis revealed greater activity for intentional than unintentional harm at an early time window (80–200 ms, 1–40 Hz) and throughout the T1–T3 time points at broadband (Fig. 1D). This occurred separately in each patient (Supplementary Table 3).

Moreover, a trial-by-trial analysis of amygdala responses (averaged during T1–T3) at broadband predicted the subjects' subsequent categorization as intentional or unintentional (Fig. 1E). Such a classification was not predicted by the activity of any other region (Supplementary Fig. 4). The amygdala was the only site that systematically discriminated between critical conditions in all subjects (at both low and high bands) and predicted their classification of events.

To examine whether such modulation in the amygdala resonated in other regions, we analysed both (i) amygdala connections during the full stimulus set presentation; and (ii) connectivity at 1–40 Hz and broadband among all recording sites at early stages. First, via a wSMI analysis (King *et al.*, 2013), we explored the integration and global broadcasting of information across non-linear amygdala connections. At relatively low frequencies (1–10 Hz), enhanced fronto-amygdalar connectivity (each subject separately: Subject 1: mesial/lateral supplementary motor area; Subject 2: orbitofrontal cortex; Subject 3: inferior frontal gyrus, pars orbitalis, lateral and posterior medial frontal gyrus; Wilcoxon, threshold of $P < 0.05$) was observed for intentional relative to unintentional harm (Fig. 2A). The evoked responses of these prefrontal regions, which presented early connectivity with the amygdala, featured late (but not early) stimulus-related modulations (Supplementary Fig. 5). We also assessed functional connectivity among all recording sites at an early window (~T1: 0–500 ms). Again, compared with unintentional harm, intentional harm induced stronger frontotemporal connectivity in all patients (bootstrapping, for 1–40 Hz: Subject 1: $P = 6.3139 \times 10^{-35}$, $t = 42.54$; Subject 2: $P = 7.989 \times 10^{-33}$, $t = 35.24$; Subject 3: $P = 2.8841 \times 10^{-10}$, $t = 21.18$; for 60–150 Hz: Subject 1: $P = 5.2694 \times 10^{-48}$, $t = 42.35$; Subject 2: $P = 1.9606 \times 10^{-11}$, $t = 32.21$; Subject 3: $P = 2.7941 \times 10^{-58}$, $t = 43.95$, see Fig. 2B), even when controlling for the neutral condition (Supplementary Fig. 6). In addition, we found that intentional harm elicited increased fronto-temporal connectivity at medium and long range distances (Supplementary Fig. 7). Thus, detection of intentional harm was associated with greater fronto-amygdala information sharing during T1–T3 and with fronto-temporal coupling at early stages (~T1).

Discussion

Previous reports pointed to the amygdala as a critical hub to appraise intentional harmful actions and stimulus salience (Treadway *et al.*, 2014). Our results provide unprecedented spatiotemporal evidence for its role in the early encoding of intention, the subsequent categorization of harmful events, and the automatic modulation of corticolimbic connections. These findings support the view that the amygdala indexes the biological significance of salient stimuli through multi-pathway networks (Pessoa and Adolphs, 2010).

The concept of intentionality has been variously defined in the literature. Here, we propose that harm is intentional insofar as it reflects the perpetrator's motivation to deliberately hurt another person, leading to mostly negative moral judgements (Supplementary material). We have selected a well-validated and replicated set of stimuli allowing an early and unambiguous categorization of intentional harm versus unintentional harm, while controlling for basic variables (such as familiarity) (Supplementary material). Future studies should assess early modulations of amygdala activity by intentionality manipulating both basic variables and other potentially relevant cognitive dimensions (Supplementary material).

The amygdala has been implicated in the processing and transmission of sensory salient stimuli to guide behaviours and decision-making (Janak and Tye, 2015). Consistent with

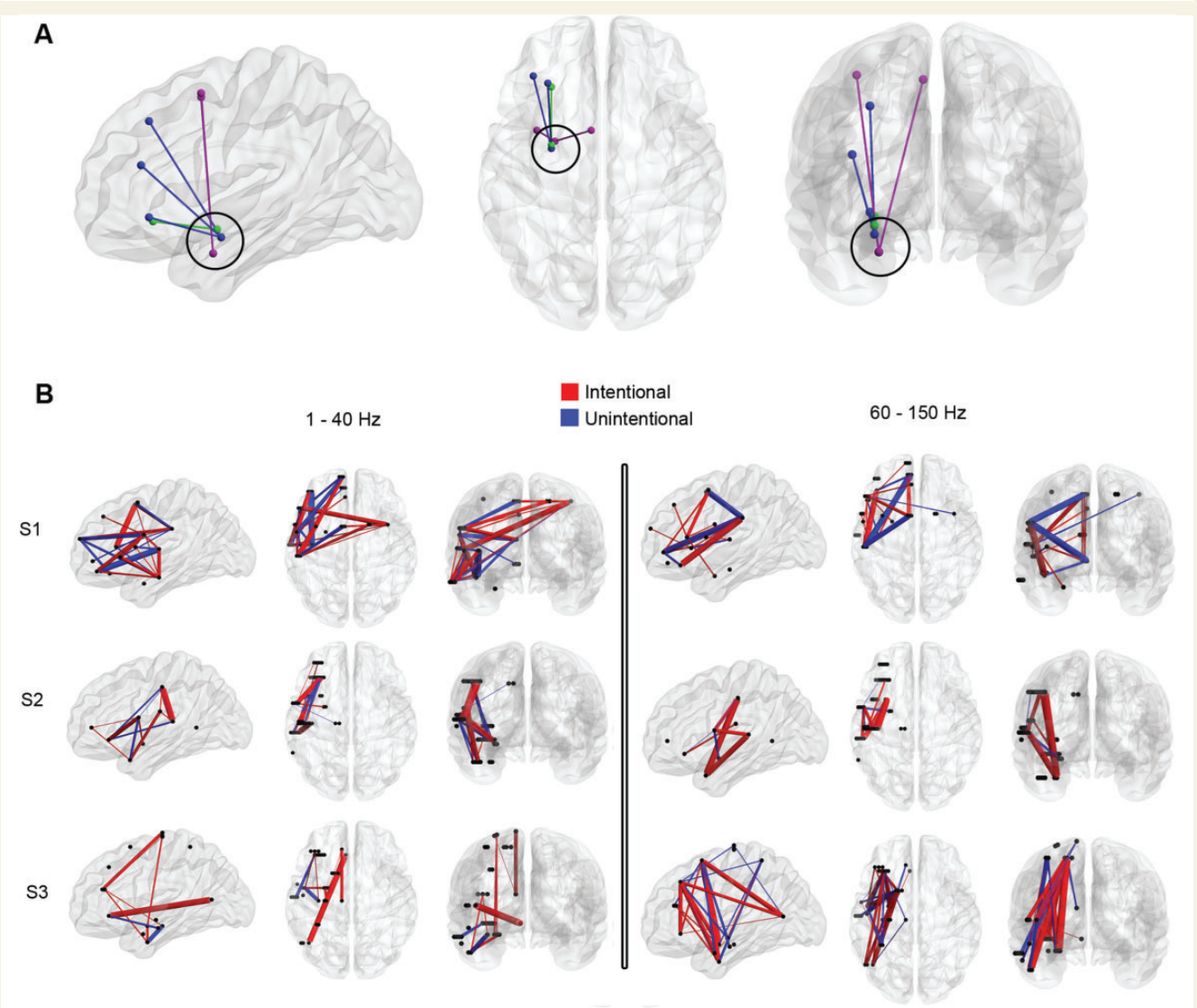

Figure 2 Corticolimbic and frontotemporal tuning of intentional actions. (**A**) WSMI. Significant connections of the amygdala with frontal regions for the intentional conditions (Wilcoxon Signed Rank Test, threshold of $P < 0.05$ for each subject). Each colour represents a different subject. (**B**) Brief Time Span Functional Connectivity. Significant correlations of intentional and unintentional conditions for each subject in a 0–500 ms window. Lines and line-widths indicate *t*-values and their absolute magnitudes, respectively. *Left*: A significantly larger number of connections (1–40 Hz) was found for the intentional conditions [$P < 0.01$ bootstrapping: Subject 1 (S1): $P = 6.3139 \times 10^{-35}$, $t = 42.54$; Subject 2 (S2): $P = 7.989 \times 10^{-33}$, $t = 35.24$; Subject 3 (S3): $P = 2.8841 \times 10^{-10}$,$t = 21.18$]. *Right*: A significantly larger number of connections (broadband) were found for the intentional conditions [Subject 1 (S1): $P = 5.2694 \times$ '10^{-48}, $t = 42.35$; Subject 2 (S2): $P = 1.9606 \times 10^{-11}$, $t = 32.21$; Subject 3 (S3): $P = 2.7941 \times 10^{-58}$, $t = 43.95$].

this claim, amygdala activity at broadband (a band that captures spike firing neurons) (Manning *et al.*, 2009) predicted single-trial behavioural performance, as previously reported for aversive learning (Lim *et al.*, 2009). The rapid (~125 ms) involvement of this structure replicates previous findings with scalp EEG (Decety and Cacioppo, 2012; Escobar *et al.*, 2014), highlighting its role in other automatic processes (Pessoa and Adolphs, 2010), such as emotional salience and face/object recognition (see Supplementary material for a deeper assessment of this finding). Note that relatively slow (Janak and Tye, 2015) and high (Oya *et al.*, 2002) amygdala frequencies are sensitive to stimulus salience modulations. The absence of similar discrimination/prediction in other associated regions corroborates the specificity of amygdala activity in intentionality attribution (Treadway *et al.*, 2014).

We also observed an early coupling of corticolimbic networks previously implicated in intentional harm processing (Treadway *et al.*, 2014) (Supplementary material). As detailed in the Supplementary material, this aligns with extant models of social cognition (Moll and Schulkin, 2009; Fumagalli and Priori, 2012; Ibanez and Manes, 2012) and fast fronto-amygdala networks (Pessoa and Adolphs, 2010). Using a novel method (wSMI) (King

et al., 2013), we showed enhanced information sharing at relatively slow (1–10 Hz) frequencies during observation of intentional actions. Because theta fronto-amygdaline oscillation is enhanced during aversive stimuli processing (Janak and Tye, 2015), this may indicate a general role for low-frequency coupling between these regions in the face of aversion-inducing events. Moreover, the early increases in frontotemporal connectivity suggest rapid spreading of amygdala boosts to other regions. Such a claim is consistent with the findings that (i) activity flows from limbic to frontal structures occur between 190–347 ms (Catenoix *et al.*, 2011); (ii) salient stimuli modulate cortical activity in early epochs (~100 ms) (Kawasaki *et al.*, 2001); causing (iii) parallel distributed frontotemporal processing (Krolak-Salmon *et al.*, 2004; Brazdil *et al.*, 2009) (Supplementary material).

Intracranial EEG recordings can provide novel and robust results (Foster *et al.*, 2015). Our results provide unprecedented spatiotemporal evidence for the role of amygdala in the early encoding of intention, the subsequent categorization of harmful events, and the automatic modulation of cortico-limbic connections, all systematically observed in each subject. Although intracranial measures provide a unique source of information that cannot be obtained through non-invasive methods, they also feature important limitations. We have carefully dealt with the well-known caveats of intracranial EEG research by adopting several precautions to minimize the effects of pathological tissue in our signals (Supplementary material). Finally, we could not presently examine laterality differences in amygdala activations, an issue that calls for further research (Supplementary material).

By overcoming the spatiotemporal limitations of previous neuroimaging studies of the amygdala, the present results help to clarify the 'many roads' view. Consistent with this perspective, we observed early amygdala responses guided by stimulus salience and rapid parallel coupling with other regions. Nevertheless, our results also highlight the amygdala's critical role in automatically encoding and classifying intentional harm during moral evaluation—functions that no other region seems to subserve.

Funding

This work was partially supported by grants from CONICET, CONICYT/FONDECYT Regular (1130920), FONCyT-PICT 2012-0412, 2012-1309, and the INECO Foundation. V.L. is sponsored by Fondecyt 1150241, M.S. is sponsored by CONICET and the James McDonnell Foundation 21st Century ScienceInitiative in Understanding Human Cognition Scholar Award.

Supplementary material

Supplementary material is available at *Brain* online.

References

Ames DL, Fiske ST. Perceived intent motivates people to magnify observed harms. Proc Natl Acad Sci USA 2015; 112: 3599–605.

Boubela RN, Kalcher K, Huf W, Seidel EM, Derntl B, Pezawas L, et al. fMRI measurements of amygdala activation are confounded by stimulus correlated signal fluctuation in nearby veins draining distant brain regions. Sci Rep 2015; 5: 10499.

Brazdil M, Roman R, Urbanek T, Chladek J, Spok D, Marecek R, et al. Neural correlates of affective picture processing–a depth ERP study. Neuroimage 2009; 47: 376–83.

Catenoix H, Magnin M, Mauguiere F, Ryvlin P. Evoked potential study of hippocampal efferent projections in the human brain. Clin Neurophysiol 2011; 122: 2488–97.

Decety J, Cacioppo S. The speed of morality: a high-density electrical neuroimaging study. J Neurophysiol 2012; 108: 3068–72.

Decety J, Cowell JM. The complex relation between morality and empathy. Trends Cogn Sci 2014; 18: 337–9.

Decety J, Michalska KJ, Kinzler KD. The contribution of emotion and cognition to moral sensitivity: a neurodevelopmental study. Cerebral Cortex. 2012; 22: 209–20.

Escobar MJ, Huepe D, Decety J, Sedeno L, Messow MK, Baez S, et al. Brain signatures of moral sensitivity in adolescents with early social deprivation. Sci Rep 2014; 4: 5354.

Foster BL, Rangarajan V, Shirer WR, Parvizi J. Intrinsic and task-dependent coupling of neuronal population activity in human parietal cortex. Neuron 2015; 86: 578–90.

Fumagalli M, Priori A. Functional and clinical neuroanatomy of morality. Brain 2012; 135(Pt 7): 2006–21.

Gross J. Analytical methods and experimental approaches for electrophysiological studies of brain oscillations. J Neurosci Methods 2014; 228: 57–66.

Huebner B, Dwyer S, Hauser M. The role of emotion in moral psychology. Trends Cogn Sci 2009; 13: 1–6.

Ibanez A, Cardona JF, Dos Santos YV, Blenkmann A, Aravena P, Roca M, et al. Motor-language coupling: direct evidence from early Parkinson's disease and intracranial cortical recordings. Cortex 2013; 49: 968–84.

Ibanez A, Manes F. Contextual social cognition and the behavioral variant of frontotemporal dementia. Neurology 2012; 78: 1354–62.

Jacobs J, Kahana MJ. Direct brain recordings fuel advances in cognitive electrophysiology. Trends Cogn Sci 2010; 14: 162–71.

Janak PH, Tye KM. From circuits to behaviour in the amygdala. Nature 2015; 517: 284–92.

Kawasaki H, Kaufman O, Damasio H, Damasio AR, Granner M, Bakken H, et al. Single-neuron responses to emotional visual stimuli recorded in human ventral prefrontal cortex. Nat Neurosci 2001; 4: 15–6.

King JR, Sitt JD, Faugeras F, Rohaut B, El Karoui I, Cohen L, et al. Information sharing in the brain indexes consciousness in noncommunicative patients. Curr Biol 2013; 23: 1914–9.

Krolak-Salmon P, Henaff MA, Vighetto A, Bertrand O, Mauguiere F. Early amygdala reaction to fear spreading in occipital, temporal, and frontal cortex: a depth electrode ERP study in human. Neuron 2004; 42: 665–76.

Lim SL, Padmala S, Pessoa L. Segregating the significant from the mundane on a moment-to-moment basis via direct and indirect amygdala contributions. Proc Natl Acad Sci USA 2009; 106: 16841–6.

Manning JR, Jacobs J, Fried I, Kahana MJ. Broadband shifts in local field potential power spectra are correlated with single-neuron spiking in humans. J Neurosci 2009; 29: 13613–20.

Moll J, Schulkin J. Social attachment and aversion in human moral cognition. Neurosci Biobehav Rev 2009; 33: 456–65.

Moll J, Zahn R, de Oliveira-Souza R, Krueger F, Grafman J. Opinion: the neural basis of human moral cognition. Nat Rev Neurosci 2005; 6: 799–809.

Naccache L, Gaillard R, Adam C, Hasboun D, Clemenceau S, Baulac M, et al. A direct intracranial record of emotions evoked by subliminal words. Proc Natl Acad Sci USA 2005; 102: 7713–7.

Omigie D, Dellacherie D, Hasboun D, George N, Clement S, Baulac M, et al. An intracranial EEG study of the neural dynamics of musical valence processing. Cereb Cortex 2015; 25: 4038–47.

Oya H, Kawasaki H, Howard MA, 3rd, Adolphs R. Electrophysiological responses in the human amygdala discriminate emotion categories of complex visual stimuli. J Neurosci 2002; 22: 9502–12.

Pessoa L, Adolphs R. Emotion processing and the amygdala: from a 'low road' to 'many roads' of evaluating biological significance. Nat Rev Neurosci 2010; 11: 773–83.

Treadway MT, Buckholtz JW, Martin JW, Jan K, Asplund CL, Ginther MR, et al. Corticolimbic gating of emotion-driven punishment. Nat Neurosci 2014; 17: 1270–5.

Tukey JW. Exploratory data analysis. Reading, MA: Addison-Wesley Pub. Co.; 1977.

Young L, Cushman F, Hauser M, Saxe R. The neural basis of the interaction between theory of mind and moral judgment. Proc Natl Acad Sci USA 2007; 104: 8235–40.